Corrected 23/05/13

Prize [2-7 June]

historical

Chapter 1

Preface

The elementary modes of nuclear excitation are vibrations and rotations, single–particle (quasiparticle) motion, and pairing vibrations and rotations. The specific reactions probing these modes are inelastic and Coulomb excitation, ~~and~~ single– and two– particle transfer processes respectively.

Pairing vibrations and rotations, closely connected with nuclear superfluidity are, arguably, a paradigm of quantal nuclear phenomena. They thus play a central role within the field of nuclear structure. It is only natural that two–nucleon ~~(Cooper pair)~~ transfer plays a similar role concerning direct nuclear reactions. In fact, this is the central subject of the present monograph.

At the basis of pairing phenomena one finds Cooper pairs, weakly bound, extended, strongly overlapping bosonic entities, made out of pairs of nucleons dressed by collective vibrations and interacting through the exchange of these vibrations as well as through the bare NN–interaction. Cooper pairs not only change the statistics of the nuclear stuff around the Fermi surface and, condensing, the properties of nuclei close to their ground state. They also display a rather remarkable mechanism of tunnelling between ~~the weakly interacting nuclei acting as~~ target and projectile in ~~a~~ direct two–nucleon transfer reaction. In fact, displaying correlations over distances (correlation length) much larger than nuclear dimensions, Cooper pairs are forced to be confined within such dimensions by the action of the average potential, which can be viewed as an external field as far as ~~Cooper~~ these pairs are concerned.

The correlation length paradigm comes into evidence, for example, when two nuclei are set into weak contact in a direct reaction. In this case, each of the partner nucleons ~~of a pair~~ has a finite probability to be confined within the mean field of the ~~target and of the projectile~~ each of the two nuclei. It is then natural that a Cooper pair can tunnel, equally well correlated, between target and projectile, through a simultaneous than through a successive transfer process. In particular, in this last case, making use of virtual states which, if forced to become real by intervening the reaction with an external mean field, will lead to single–nucleon transfer processes. The above mentioned weak coupling Cooper pair tunnelling reminds ~~to~~ the tunnelling mechanism of ~~electron~~ electronic Cooper pairs across a barrier (e.g. a dioxide layer) separating two superconductors, known as Josephson junction. The main difference is that, as a rule, in the nuclear time dependent junction provided by a direct two–nucleon transfer process, only one or even none of the two weakly interacting nuclei are superfluid (or superconducting). Now, in nuclei, paradigmatic example of fermionic finite many–body system, zero point fluctuation (ZPF) in general, and those associated with pair addition and pair substraction modes known as pairing vibrations in particular, are much stronger than in condensed matter. Consequently, and in keeping with the fact that pairing vibrations are the nuclear embodiment of Cooper pairs in nuclei, pairing correlations based on even a single Cooper pair lead to clearly observable effects. In some cases, like for example in connection with the exotic nucleus ^{11}Li, to a tenuous halo extending much beyond standard nuclear dimensions.

Cooper pair tunneling has played and is playing a central role in the probing of these subtle quantal phenomena, both in the case of exotic nuclei as well as of nuclei lying along the stability valley, and have been instrumental in shedding light on the subject of pairing in nuclei at large, and on nuclear superfluidity in particular. Consequently, the subject of two–nucleon transfer occupies ~~they occupy~~ a central place in the present monograph both concerning the conceptual and the computational aspects of the description of nuclear pairing, as well as regarding the quantitative confrontation of the results and predictions with the experimental findings.

Because the interweaving of the variety of elementary modes of nuclear excitation, the study of Cooper pair tunnelling in nuclei, involves also the description of one–nucleon transfer as well as knock out processes, let alone inelastic and Coulomb excitation processes.

The corresponding softwares COOPER, ONE, KNOCK, INELASTIC and COULOMB are briefly presented, referring to the enclosed CD for the corresponding files and input–output examples.

Summing up, general physical arguments and technical computational details, as well as the software used in the description and calculation of the absolute two–nucleon transfer cross sections, making use of state of the art nuclear structure information, are provided. As a consequence, theoretical and experimental practitioners, as well as PhD students could use the present monograph,

, at profit,

aside from requiring a consistent desciption of nuclear structure in terms of dressed quasiparticles and vibrations, resuting from both bare and induced interactions,

Questions Ch. 6

Throughout:

larger characters, in particular concerning the formulae

One can hardly see ~~that~~ in Eq. (6.6)

p. 4 $\psi^{J_f}_{m_f}(r_{An}, \sigma) = \ldots \quad [\;\;]_{l_i m_i}$ (6.6)

make size such ~~that~~ the subindices of subindices like and can be clearly seen (not only in the screen, but in the printed page)

p. 5 eq. (6.14)

$$[\chi(-\sigma)\chi(\sigma)]^0_0$$

from the rest of the page one can see ~~that~~ you interpret σ as a magnetic quantum number i.e. $\sigma = \pm 1/2$. In ~~fact~~, you

II

write in (6.13) p. 5

$$\left\{ \left[Y^{\ell_f}(\hat{r}_{An}) \mathcal{X}^{1/2}(-\sigma) \right]^{J_F} \mathcal{O}_F \left[Y^{\ell_i}(\hat{r}_{bn}) \mathcal{X}^{1/2}(\sigma) \right]^{J_i} \right\}^{P}_{m_i - m_f}$$

now when you couple you sum over magnetic q. number, thus you do not write them within brackets, e.g. But you do it concerning the spin function

~~Suggestion, ei the~~ ~~This~~ ~~Suggestion~~, The standard ~~[illegible]~~ notation for spin wavefunctions is $\mathcal{X}^{\sigma}_{m_\sigma}$, ~~[illegible]~~ where $\sigma = 1/2$ and $m_\sigma = \pm 1/2$. Now we can also use

$$\mathcal{X}^{1/2}(\sigma)$$

and define σ as the magnetic quantum number of the spin

In any case

$$[\mathcal{X}(-\sigma)\,\mathcal{X}(\sigma)]^0_0 \text{ is wrong and}$$

you should write

$$[\mathcal{X}^{1/2}\,\mathcal{X}^{1/2}]^0_0$$

In fact, if one goes to

(III)

equation (7.1) of your notes on two-particle transfer (7.1 simultaneous transfer 7.1.1 distorted waves) you write

$$\chi_{m_i}(\sigma_p)$$

~~which means that~~

~~[illegible]~~ which means ~~that~~ σ is the spin variable, like the coordinate in $Y^{l_i}_{m_i}(\hat{R})$ and ~~that~~ $\chi \equiv \chi^{1/2}$

Thus, let us use the notation

$$\Rightarrow \boxed{\boxed{\chi_m(\sigma)}} \left(\equiv \chi^{1/2}_m(\sigma)\right)$$

~~throughout~~.

See e.g. Eq. (7.7) p. 3 ~~[illegible]~~ your notes 2n-transfer. Last line you write

$$[\chi(\sigma_1)\chi(\sigma_2)]^0_0$$

Chapter 6

One-particle transfer

Write all references as they are written, ~~Not~~ not as reference but as e.g. in p. 18 (cf. e.g. Brauh and Broglia - - - - -)

Also Figs. + Captions

text
slightly larger characters please !!

texto
letras un poco mas grandes por favor

Chapter 6

One–particle transfer

leading to modified formfactors *) resulting from the interweaving of a number of orbitals with the original, unperturbed single-particle state

In what follows we present a derivation of the one–particle transfer differential cross section within the framework of the DWBA.

The structure input for the calculations are mean field potentials and single–particle states, dressed through the coupling with the variety of collective, (quasi) bosonic nuclear degrees of freedom. With the help of these ~~elements~~, and of optical potentials, one can calculate the absolute differential cross sections, quantities which can ~~be~~ directly be compared with the experimental findings.

modified formfactors

In this way one avoids to introduce, let alone use spectroscopic factors, quantities which are rather elusive to define. This is in keeping with the fact that as a nucleon moves through the nucleus it feels the presence of the other nucleons whose configurations change as time proceeds. It takes time for this information to be fed back on the nucleon. This renders the average potential nonlocal in time. A time–dependent operator can always be transformed into an energy dependent operator, implying an ω–dependence of the properties which are usually adscribed to particles like (effective) mass, charge, etc. Furthermore, due to the Pauli principle, the average potential is also non local in space (cf. App. 6.A. and 6.B) Consequently, one is forced to deal with nucleons which carry around a cloud of (quasi) bosons, aside from ~~continuously and instantaneously~~ exchanging its position with that of the other nucleons. It is of notice that the above ~~questions~~ mentioned phenomena are not only found within the realm of nuclear physics, but are common within the framework of many–body systems as well as field theories like quantum electrodynamic (QED). In fact, a basic result of such theories is that nothing is free. A textbook example ~~is~~ being provided by the Lamb shift, resulting from the dressing of the hydrogen atom electron, as a result of the exchange of ~~such~~ this electron with those participating in the spontaneous, virtual excitation ~~(ZPF)~~ (zero point fluctuations (ZPF)) of the QED vacuum (cf. App. 6.C).

Within this context see Sect. 6.2 (Examples and Applications) concerning e.g. the phenomenon of parity inversion in N=6 (closed shell) exotic halo nuclei (cf. Fig. 6.1).

6.1 General derivation

We ~~want~~ (proceed now) to derive the transition amplitude for the reaction

$$A + a(= b + 1) \longrightarrow B(= A + 1) + b, \tag{6.1}$$

(for a simplified derivation cf. App D).

*) It is of notice that single-particle modified formfactors have their counterpart in the transition densities (Ch. 5) and in the modified two-nucleon modified formfactors (Chs. 7 and 8) associated with inelastic and pair transfer, respectively.

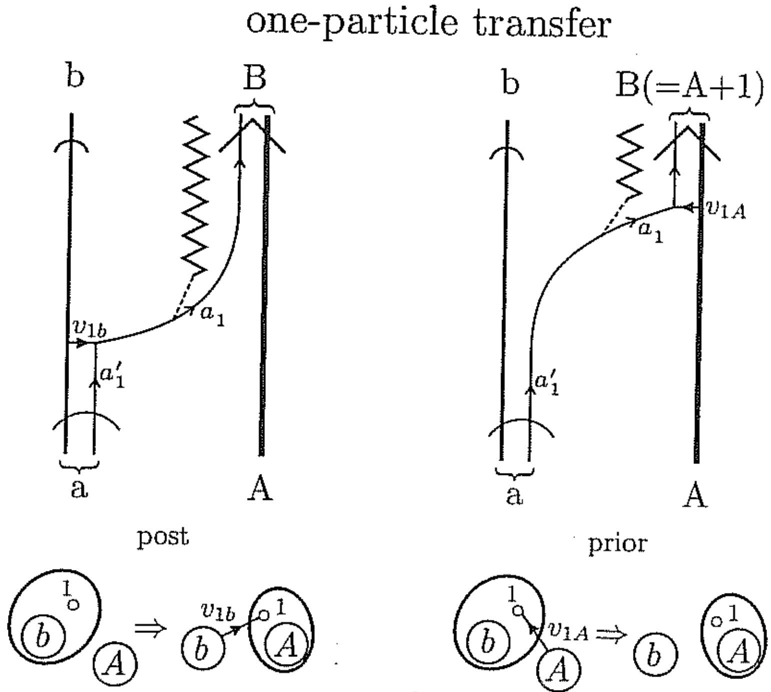

Figure ~~6.3:~~ 6.1

One-particle transfer reaction

$a(=b+1)+A \rightarrow b+B(=A+1)$.

The time arrow is assumed to point upwards. The quantum numbers characterizing the states in which the transferred nucleon moves in projectile and target are denoted a'_1 and a_1 respectively. The interaction inducing the nucleon to be transferred can act either in the entrance channel ((a,A); v_{1A}), prior representation) or in the exit channel ((b,B); v_{1b}), post representation), in keeping with energy conservation. In the transfer process, the nucleon changes orbital at the same time ~~that~~ a change in the mass partition takes place. The corresponding relative motion missmatch is known as the recoil process, and is represented by a jagged line which provides information on the evolution of r_{1A} (r_{1b}). In other words on the coupling of reaction and transfer modes,

(4)

Letras más grandes

and the the nucleon

Let us assume that the nucleon bound initially to the core b is in a single–particle state with orbital and total angular momentum l_i and j_i respectively, and that in the final state (bound to core A) it is in l_f, j_f state. The total spin and magnetic quantum numbers of nuclei A, a, B, b are $\{J_A, M_A\}$, $\{J_a, M_a\}$, $\{J_B, M_B\}$, $\{J_b, M_b\}$. Denoting ξ_A and ξ_b the intrinsic wavefunctions describing the structure of nuclei A and b respectively, and $\mathbf{r}_{An}$ and $\mathbf{r}_{bn}$ the relative coordinates of the transferred nucleon with respect to the CM of nuclei A and b respectively, one can write the wavefunctions of the colliding nuclei A, a as

respectively

coordinates of the

"intrinsic"

$$\begin{aligned}
&\phi^{J_A}_{M_A}(\xi_A),\\
&\Psi(\xi_b, \mathbf{r}_{b1}) = \sum_{m_i} \langle J_b\ j_i\ M_b\ m_i | J_a\ M_a\rangle \phi^{J_b}_{M_b}(\xi_b)\psi^{j_i}_{m_i}(\mathbf{r}_{bn}, \sigma),
\end{aligned} \tag{6.2}$$

while the "intrinsic" wavefunctions describing the structure of nuclei B and b are

$$\begin{aligned}
&\phi^{J_b}_{M_b}(\xi_b),\\
&\Psi(\xi_A, \mathbf{r}_{A1}) = \sum_{m_f} \langle J_A\ j_f\ M_A\ m_f | J_B\ M_B\rangle \phi^{J_A}_{M_A}(\xi_A)\psi^{j_f}_{m_f}(\mathbf{r}_{An}, \sigma).
\end{aligned} \tag{6.3}$$

measure e

For an unpolarized incident beam (sum over M_A, M_a and dividing by $(2J_A+1)$, $(2J_a+1)$) and assuming that one does not detect the final polarization (sum over M_B, M_b), the differential cross section in the DWBA can be written as

$$\begin{aligned}
\frac{d\sigma}{d\Omega} &= \frac{k_f}{k_i}\frac{\mu_i\mu_f}{4\pi^2\hbar^4}\frac{1}{(2J_A+1)(2J_a+1)}\\
&\times \sum_{\substack{M_A, M_a\\ M_B, M_b}} \left| \sum_{m_i, m_f} \langle J_b\ j_i\ M_b\ m_i | J_a\ M_a\rangle \langle J_A\ j_f\ M_A\ m_f | J_B\ M_B\rangle T_{m_i, m_f} \right|^2 .
\end{aligned} \tag{6.4}$$

is the single-particle wavefunction describing the motion of the nucleon to be transferred, in the initial state. Similarly for $\psi^{j_f}_{m_f}$.

The transition amplitude T_{m_i, m_f} is

$$T_{m_i, m_f} = \sum_\sigma \int d\mathbf{r}_f d\mathbf{r}_{bn} \chi^{(-)*}(\mathbf{r}_f)\psi^{j_f *}_{m_f}(\mathbf{r}_{An}, \sigma) V(r_{bn}) \psi^{j_i}_{m_i}(\mathbf{r}_{bn}, \sigma)\chi^{(+)}(\mathbf{r}_i), \tag{6.5}$$

where

$$\psi^{j_i}_{m_i}(\mathbf{r}_{An}, \sigma) = u_{j_i}(r_{bn}) \left[Y^{l_i}(\hat{r}_i)\chi(\sigma)\right]_{j_i m_i}, \tag{6.6}$$

The incoming and outgoing distorted waves are

$e^{i\sigma'}$ y no $e^{-i\sigma'}$ si pones $\chi^{(-)*}$

$$\chi^{(+)}(\mathbf{k}_i, \mathbf{r}_i) = \frac{4\pi}{k_i r_i} \sum_{l'} i^{l'} e^{i\sigma_{l'}} g_{l'}(\hat{r}_i) \left[Y^{l'}(\hat{r}_i)Y^{l'}(\hat{k}_i)\right]^0_0, \tag{6.7}$$

no entiendo porqué

letras mas grandes por favor

and

$$\chi^{(-)*}(\mathbf{k}_f, \mathbf{r}_f) = \frac{4\pi}{k_f r_f} \sum_l i^{-l} e^{i\sigma_l} f_l(\hat{r}_f) \left[Y^l(\hat{r}_f)Y^l(\hat{k}_f)\right]^0_0, \tag{6.8}$$

respectively. Now,

no poner el complejo conjugado

$$\begin{aligned}
\left[Y^l(\hat{r}_f)Y^l(\hat{k}_f)\right]^0_0 \left[Y^{l'}(\hat{r}_i)Y^{l'}(\hat{k}_i)\right]^0_0 &= \sum_K ((ll)_0(l'l')_0|(ll')_K(ll')_K)_0\\
&\times \left\{\left[Y^l(\hat{r}_f)Y^{l'}(\hat{r}_i)\right]^K \left[Y^l(\hat{k}_f)Y^{l'}(\hat{k}_i)\right]^K\right\}^0_0 .
\end{aligned} \tag{6.9}$$

$$\psi^{j_f *}_{m_f}(\vec{r}_{An},\sigma) = (-1)^{j_f-m_f}\psi^{j_f}_{-m_f}(\vec{r}_{An},\sigma)$$

5

because of jm rappresentation neither the m component of the ~~orbital angular momentum~~ nor that of the spin should appear

6.1. GENERAL DERIVATION

The 9j symbol can be explicitly evaluated to ~~be~~ give,

$$((ll)_0(l'l')_0|(ll')_K(ll')_K)_0 = \sqrt{\frac{2K+1}{(2l+1)(2l'+1)}}, \tag{6.10}$$

while

~~and the angular momenta coupling is~~

write

$$\left\{\left[Y^l(\hat{r}_f)Y^{l'}(\hat{r}_i)\right]^K\left[Y^l(\hat{k}_f)Y^{l'}(\hat{k}_i)\right]^K\right\}^0_0 = \sum_M \langle K\,K\,M\,-M|0\,0\rangle\left[Y^l(\hat{r}_f)Y^{l'}(\hat{r}_i)\right]^K_M$$
$$\times\left[Y^l(\hat{k}_f)Y^{l'}(\hat{k}_i)\right]^K_{-M} = \sum_M \frac{(-1)^{K+M}}{\sqrt{2K+1}}\left[Y^l(\hat{r}_f)Y^{l'}(\hat{r}_i)\right]^K_M\left[Y^l(\hat{k}_f)Y^{l'}(\hat{k}_i)\right]^K_{-M}. \tag{6.11}$$

$-m_\sigma$ or $-m_s$

Thus,

$$\left[Y^l(\hat{r}_f)Y^l(\hat{k}_f)\right]^0_0\left[Y^{l'}(\hat{r}_i)Y^{l'}(\hat{k}_i)\right]^0_0 =$$
$$\sum_{K,M}\frac{(-1)^{K+M}}{\sqrt{(2l+1)(2l'+1)}}\left[Y^l(\hat{r}_f)Y^{l'}(\hat{r}_i)\right]^K_M\left[Y^l(\hat{k}_f)Y^{l'}(\hat{k}_i)\right]^K_{-M}. \tag{6.12}$$

over which one integrates

For the angular integral to be different from zero, the integrand must be coupled to zero angular momentum (scalar). Noting that the only ~~integrated~~ variables in the ~~above~~ expression are $\hat{r}_i, \hat{r}_f$, we have to couple the remaining functions of the angular variables, namely the wavefunctions $\psi^{j_f*}_{m_f}(\mathbf{r}_{An},\sigma) = (-1)^{j_f-m_f}\psi^{j_f}_{-m_f}(\mathbf{r}_{An},-\sigma)$ and $\psi^{j_i}_{m_i}(\mathbf{r}_{bn},\sigma)$ to angular momentum K, as well as to fulfill $M = m_f - m_i$. Let us then consider

σ is the spin projection one should call m_s or m_σ,

(6.5)

$$(-1)^{j_f-m_f}\psi^{j_f}_{-m_f}(\mathbf{r}_{An},-\sigma)\psi^{j_i}_{m_i}(\mathbf{r}_{bn},\sigma) = (-1)^{j_f-m_f}u_{j_f}(r_{An})u_{j_i}(r_{bn})$$
$$\times\sum_P\langle j_f\,j_i\,-m_f\,m_i|P\,m_i-m_f\rangle\left\{\left[Y^{l_f}(\hat{r}_{An})\chi^{1/2}(-\sigma)\right]^{j_f}\left[Y^{l_i}(\hat{r}_{bn})\chi^{1/2}(\sigma)\right]^{j_i}\right\}^P_{m_i-m_f}. \tag{6.13}$$

??

?

Recoupling the spherical harmonics to angular momentum K and the spinors to $S = 0$, only one term survives the angular integral in ~~6.5~~ Eq. (6.5), namely

$$(-1)^{j_f-m_f}u_{j_f}(r_{An})u_{j_i}(r_{bn})((l_f\tfrac{1}{2})_{j_f}(l_i\tfrac{1}{2})_{j_i}|(l_fl_i)_K(\tfrac{1}{2}\tfrac{1}{2})_0)_K$$
$$\times\langle j_f\,j_i\,-m_f\,m_i|K\,m_i-m_f\rangle\left[Y^{l_f}(\hat{r}_{An})Y^{l_i}(\hat{r}_{bn})\right]^K_{m_i-m_f}[\chi(-\sigma)\chi(\sigma)]^0_0. \tag{6.14}$$

gregory $\sigma = 1/2$ (m_s) $m_\sigma = \pm 1/2$ in any case, within $[\;\;]^0_0$ one cannot specify the magnetic quantum number

Because ~~Making use of the fact that~~ the sum over spins yields a factor $-\sqrt{2}$, and in keeping with the fact that $M = m_f - m_i$, one obtains,

$$T_{m_i,m_f} = (-1)^{j_f-m_f}\frac{-16\sqrt{2}\pi^2}{k_fk_i}\sum_{ll'} i^{l'-l}e^{\sigma^l_f+\sigma^{l'}_i}\sum_K((l_f\tfrac{1}{2})_{j_f}(l_i\tfrac{1}{2})_{j_i}|(l_fl_i)_K(\tfrac{1}{2}\tfrac{1}{2})_0)_K$$
$$\times\langle j_f\,j_i\,-m_f\,m_i|K\,m_i-m_f\rangle\left[Y^l(\hat{k}_f)Y^{l'}(\hat{k}_i)\right]^K_{m_i-m_f}\int d\mathbf{r}_f d\mathbf{r}_{bn}\frac{f_l(r_f)g_{l'}(r_i)}{r_fr_i}$$
$$\times u_{j_f}(r_{An})u_{j_i}(r_{bn})V(r_{bn})(-1)^{K+m_f-m_i}\left[Y^l(\hat{r}_f)Y^{l'}(\hat{r}_i)\right]^K_{m_f-m_i}\left[Y^{l_f}(\hat{r}_{An})Y^{l_i}(\hat{r}_{bn})\right]^K_{m_i-m_f}. \tag{6.15}$$

$$\chi^{1/2}(-\sigma) \Rightarrow \chi^{1/2}(-m_s)$$

(6)

Again, the only term of the expression

$$(-1)^{K+m_f-m_i}\left[Y^l(\hat r_f)Y^{l'}(\hat r_i)\right]^K_{m_f-m_i}\left[Y^{l_f}(\hat r_{An})Y^{l_i}(\hat r_{bn})\right]^K_{m_i-m_f}=$$

$$(-1)^{K+m_f-m_i}\sum_P\langle K\;K\;m_f-m_i\;m_i-m_f|P\;0\rangle\left\{\left[Y^l(\hat r_f)Y^{l'}(\hat r_i)\right]^K\left[Y^{l_f}(\hat r_{An})Y^{l_i}(\hat r_{bn})\right]^K\right\}^P_0$$

which ~~survives~~ remains after angular integration is the one with $P=0$, that is,

$$\frac{1}{\sqrt{(2K+1)}}\left\{\left[Y^l(\hat r_f)Y^{l'}(\hat r_i)\right]^K\left[Y^{l_f}(\hat r_{An})Y^{l_i}(\hat r_{bn})\right]^K\right\}^0_0=$$

$$\frac{1}{\sqrt{(2K+1)}}\sum_{M_K}\langle K\;K\;M_K\;-M_K|0\;0\rangle\left[Y^l(\hat r_f)Y^{l'}(\hat r_i)\right]^K_{M_K}$$

$$\times\left[Y^{l_f}(\hat r_{An})Y^{l_i}(\hat r_{bn})\right]^K_{-M_K}=\frac{1}{\sqrt{(2K+1)}}\sum_{M_K}\frac{(-1)^{K+M_K}}{\sqrt{(2K+1)}}\left[Y^l(\hat r_f)Y^{l'}(\hat r_i)\right]^K_{M_K}$$

$$\times\left[Y^{l_f}(\hat r_{An})Y^{l_i}(\hat r_{bn})\right]^K_{-M_K}=$$

Consequently,

$$\frac{1}{2K+1}\sum_{M_K}(-1)^{K+M_K}\left[Y^l(\hat r_f)Y^{l'}(\hat r_i)\right]^K_{M_K}\left[Y^{l_f}(\hat r_{An})Y^{l_i}(\hat r_{bn})\right]^K_{-M_K},$$

Fig. 6.2 (2)

an expression which is spherically symmetric. One can evaluate it for a particular configuration, ~~in particular~~ e.g. setting $\hat r_f=\hat z$ and the center of mass A,b,n in the $x-z$ plane (see Fig. 6.2). Once the orientation in space of this "standard" configuration is specified (~~with~~, for example, a rotation $0\le\alpha\le2\pi$ around $\hat z$, a rotation $0\le\beta\le\pi$ around the new x axis and a rotation $0\le\gamma\le2\pi$ around $\hat r_{bB}$), the only ~~remaining~~ angular coordinate which remains is θ, ~~while~~ though the integral over the other three angles yields a factor $8\pi^2$. Setting $\hat r_f=\hat z$ one ~~obtains~~ can write,

$$\left[Y^l(\hat r_f)Y^{l'}(\hat r_i)\right]^K_{M_K}=\langle l\;l'\;0\;M_K|K\;M_K\rangle\sqrt{\frac{2l+1}{4\pi}}Y^{l'}_{M_K}(\hat r_i).\tag{6.16}$$

Because of $M=m_i-m_f$ and $m=m_f$, $T_{m_i,m_f}\equiv T_{m,M}$, where

$$T_{m,M}=(-1)^{j_f-m}\frac{-64\sqrt{2}\pi^{7/2}}{k_fk_i}\sum_{ll'}i^{l'-l}e^{\sigma^l_f+\sigma^{l'}_i}\sqrt{2l+1}\sum_K\frac{(-1)^K}{2K+1}((l_f\tfrac12)_{j_f}(l_i\tfrac12)_{j_i}|(l_fl_i)_K(\tfrac12\tfrac12)_0)_K$$
$$\times\langle j_f\;j_i\;-m\;M+m|K\;M\rangle\left[Y^l(\hat k_f)Y^{l'}(\hat k_i)\right]^K_M\int d\mathbf{r}_fd\mathbf{r}_{bn}\frac{f_l(r_f)g_{l'}(r_i)}{r_fr_i}$$
$$\times u_{j_f}(r_{An})u_{j_i}(r_{bn})V(r_{bn})\sum_{M_K}(-1)^{M_K}\langle l\;l'\;0\;M_K|K\;M_K\rangle\left[Y^{l_f}(\hat r_{An})Y^{l_i}(\hat r_{bn})\right]^K_{-M_K}Y^{l'}_{M_K}(\hat r_i).\tag{6.17}$$

We now turn our attention to the sum

$$\sum_{\substack{M_A,M_a\\M_B,M_b}}\left|\sum_{m,M}\langle J_b\;j_i\;M_b\;m_i|J_a\;M_a\rangle\langle J_A\;j_f\;M_A\;m_f|J_B\;M_B\rangle T_{m,M}\right|^2,\tag{6.18}$$

7

appearing

~~found~~ in the expression for the differential cross section (6.4). For any given value m', M' of m, M, ~~the sum will be~~ one finds,

$$\sum_{M_a, M_b} |\langle J_b\ j_i\ M_b\ m_i|J_a\ M_a\rangle|^2 \sum_{M_A, M_B} \left|\langle J_A\ j_f\ M_A\ m_f|J_B\ M_B\rangle\right|^2 \left|T_{m',M'}\right|^2 =$$

$$\frac{(2J_a+1)(2J_B+1)}{(2j_i+1)(2j_f+1)} \sum_{M_a, M_b} |\langle J_b\ J_a\ M_b\ -M_a|j_i\ m_i\rangle|^2$$

$$\times \sum_{M_A, M_B} \left|\langle J_A\ J_B\ M_A\ -M_B|j_f\ m_f\rangle\right|^2 \left|T_{m',M'}\right|^2, \qquad (6.19)$$

where used was made ~~by virtue~~ of the symmetry property ~~of Clebsch–Gordan coefficients.~~

$$\langle J_b\ j_i\ M_b\ m_i|J_a\ M_a\rangle = (-1)^{J_b-M_b}\sqrt{\frac{(2J_a+1)}{(2j_i+1)}}\langle J_b\ J_a\ M_b\ -M_a|j_i\ m_i\rangle_a, \qquad (6.20)$$

of the recoupling coefficients.

The sum over the Clebsch–Gordan coefficients in (6.19)is one, so (6.18) is just

$$\frac{(2J_a+1)(2J_B+1)}{(2j_i+1)(2j_f+1)} \sum_{m,M} \left|T_{m,M}\right|^2, \qquad (6.21)$$

and the differential cross section turns out to be

$$\frac{d\sigma}{d\Omega} = \frac{k_f}{k_i}\frac{\mu_i\mu_f}{4\pi^2\hbar^4}\frac{(2J_B+1)}{(2j_i+1)(2j_f+1)(2J_A+1)}\sum_{m,M}\left|T_{m,M}\right|^2, \qquad (6.22)$$

where

$$T_{m,M} = \sum_{Kll'}(-1)^{-m}\langle j_f\ j_i\ -m\ M+m|K\ M\rangle \left[Y^l(\hat{k}_f)Y^{l'}(\hat{k}_i)\right]^K_M t^K_{ll'}. \qquad (6.23)$$

Orienting $\hat{k}_i$ along the incident z direction, leads to,

$$\left[Y^l(\hat{k}_f)Y^{l'}(\hat{k}_i)\right]^K_M = \langle l\ l'\ M\ 0|K\ M\rangle\sqrt{\frac{2l'+1}{4\pi}}Y^l_M(\hat{k}_f). \qquad (6.24)$$

~~and~~ Consequently,

$$T_{m,M} = \sum_{Kll'}(-1)^{-m}\langle l\ l'\ M\ 0|K\ M\rangle\langle j_f\ j_i\ -m\ M+m|K\ M\rangle Y^l_M(\hat{k}_f)\, t^K_{ll'}, \qquad (6.25)$$

with

$$t^K_{ll'} = (-1)^{K+j_f}\frac{-32\sqrt{2}\pi^3}{k_fk_i}i^{l'-l}e^{\sigma^l_f+\sigma^{l'}_i}\frac{\sqrt{(2l+1)(2l'+1)}}{2K+1}((l_f\tfrac{1}{2})_{j_f}(l_i\tfrac{1}{2})_{j_i}|(l_fl_i)_K(\tfrac{1}{2}\tfrac{1}{2})_0)_K$$

$$\times\int dr_f\,dr_{bn}d\theta r^2_{bn}\sin\theta\, r_f\frac{f_l(r_f)g_{l'}(r_i)}{r_i}u_{j_f}(r_{An})u_{j_i}(r_{bn})V(r_{bn})$$

$$\times\sum_{M_K}(-1)^{M_K}\langle l\ l'\ 0\ M_K|K\ M_K\rangle\left[Y^{l_f}(\hat{r}_{An})Y^{l_i}(\hat{r}_{bn})\right]^K_{-M_K}Y^{l'}_{M_K}(\hat{r}_i). \qquad (6.26)$$

(8)

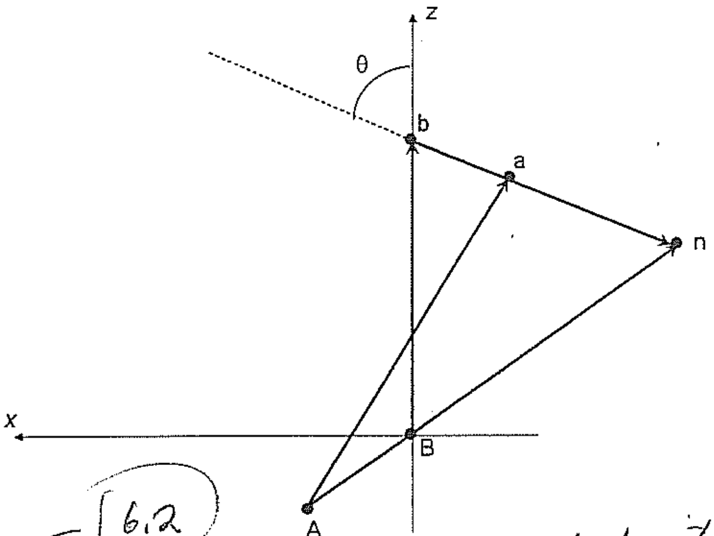

2 — 6.2

connected with

Figure 6.~~1~~: Coordinate system ~~in~~ the "standard" configuration. Note that $\mathbf{r}_f \equiv \mathbf{r}_{Bb}$, and $\mathbf{r}_i \equiv \mathbf{r}_{Aa}$.

6.1.1 Coordinates

and written

To perform the integral in (6.26), one needs the expression of $r_i, r_{An}, \hat{r}_{An}, \hat{r}_{bn}, \hat{r}_i$ in terms of the integration variables r_f, r_{bn}, θ.Because one is interested in evaluating these quantities in the particular configuration depicted in Fig. ~~6.2~~ 6.2, one has

$$\mathbf{r}_f = r_f \hat{z}, \tag{6.27}$$

$$\mathbf{r}_{bn} = -r_{bn}(\sin\theta\,\hat{x} + \cos\theta\,\hat{z}), \tag{6.28}$$

$$\mathbf{r}_{Bn} = \mathbf{r}_f + \mathbf{r}_{bn} = -r_{bn}\sin\theta\,\hat{x} + (r_f - r_{bn}\cos\theta)\,\hat{z}. \tag{6.29}$$

One can then write

$$\mathbf{r}_{An} = \frac{A+1}{A}\mathbf{r}_{Bn} = -\frac{A+1}{A} r_{bn}\sin\theta\,\hat{x} + \frac{A+1}{A}(r_f - r_{bn}\cos\theta)\,\hat{z}, \tag{6.30}$$

$$\mathbf{r}_{an} = \frac{b}{b+1}\mathbf{r}_{bn} = -\frac{b}{b+1} r_{bn}(\sin\theta\,\hat{x} + \cos\theta\,\hat{z}), \tag{6.31}$$

and

$$\mathbf{r}_i = \mathbf{r}_{An} - \mathbf{r}_{an} = -\frac{2A+1}{(A+1)A} r_{bn}\sin\theta\,\hat{x} + \left(\frac{A+1}{A} r_f - \frac{2A+1}{(A+1)A} r_{bn}\cos\theta\right)\hat{z}, \tag{6.32}$$

where A, b are the number of nucleons of nuclei A and b respectively.

6.1.2

~~6.2~~ Zero-range approximation

In the zero range approximation,

$$\int dr_{bn} r_{bn}^2 u_{j_i}(r_{bn}) V(r_{bn}) = D_0; \quad u_{j_i}(r_{bn}) V(r_{bn}) = \delta(r_{bn})/r_{bn}^2. \tag{6.33}$$

(9)

2

Fig. 6.2

It can be shown (see Fig. 6.~~?~~) that for $r_{bn} = 0$,

$$\mathbf{r}_{An} = \frac{m_A + 1}{m_A}\mathbf{r}_f \tag{6.34}$$

and —

$$\mathbf{r}_i = \frac{m_A + 1}{m_A}\mathbf{r}_f.$$

One then obtains

$$\begin{aligned} t_{ll'}^{K} = &\frac{-16\sqrt{2}\pi^2}{k_f k_i}(-1)^K \frac{D_0}{\alpha} i^{l'-l} e^{\sigma_f^l + \sigma_i^{l'}} \frac{\sqrt{(2l+1)(2l'+1)(2l_i+1)(2l_f+1)}}{2K+1} ((l_f \tfrac{1}{2})_{j_f} (l_i \tfrac{1}{2})_{j_i} | (l_f l_i)_K (\tfrac{1}{2}\tfrac{1}{2})_0)_K \\ &\times \langle l\, l'\, 0\, 0 | K\, 0\rangle \langle l_f\, l_i\, 0\, 0 | K\, 0\rangle \int dr_f\, f_l(r_f) g_{l'}(\alpha r_f) u_{j_f}(\alpha r_f), \end{aligned} \tag{6.35}$$

where

$$\alpha = \frac{A+1}{A}. \tag{6.36}$$

letras más grandes

No se ven los subindices de los subindices

~~6.5~~ 6.2 Examples and applications

In this section we discuss some examples which illustrate the workings of single-particle transfer processes at large, and in particular the flavour of the limitations by which nuclear structure studies suffer, when this specific probe to study quasiparticle properties is not operative. Let us in fact start with such an example

6.2.1 Dressing of single-particle states: parity inversion and the N=6 shell closure

- ~~$^{132}\mathrm{Sn}(d,p)^{133}\mathrm{Sn}$~~
- ~~$^{120}\mathrm{Sn}(d,p)^{121}\mathrm{Sn}$~~
- ~~$^{120}\mathrm{Sn}(p,d)^{119}\mathrm{Sn}$~~

one has recalculated again the $^{A+2}$Sn$(p,t)^{A}$Sn(gs) absolute differential cross sections. The corresponding results in comparison with the experimental data,[35] are also displayed in Fig.4. Again, in this case, theory accounts for the experimental findings within errors (see also Table 1 of the contribution of Broglia to this Volume). Also shown in Fig. 4 are the absolute differential cross sections associated with the ^{206}Pb (t,p) and ^{208}Pb$(^{16}$O,^{18}O) excitation of the pair removal mode of Pb 208, calculated making use of RPA wavefunctions (two–nucleon spectroscopic amplitudes, cf.[21] and references therein), and of global optical parameters . Theory again provides a quantitative account of the data. From the results displayed in Fig. 4, it seems fair to posit that two–nucleon transfer reaction theory has reached a quantitative level.

Within this context, it is of notice that many groups have contributed through the years to develop the reaction theory of two–nucleon transfer processes including simultaneous, successive and non–orthogonality contributions into a tool to calculate the absolute differential cross sections which can be directly compared with the experiment findings (see[36,39–49] and refs. therein; see also the Chapter of Thompson in this Volume).

5.1. *Hindsight*

BCS theory, arguably like QED, belongs to a class of descriptions of physical phenomena which come close to certainty. This is not so much because they can be microscopically derived from the ground up without free parameters or divergences -think only on G and E_{cutoff} in the first case and of renormalization in the second- but primarily because of the wide variety of phenomena they can correlate, the Josephson effect and the Lamb shift providing textbook examples. Not only this, but also the fact that they contribute paradigms which carry over other fields of research not thought of in the first time.

Because the BCS spectroscopic amplitudes describing the two–nucleon transfer process along a pairing rotational band associated with the valence orbitals can be considered essentially "exact", together with the fact that global studies of elastic scattering have lead to reliable optical model parameters for the different channels involved, it is possible to test the nuclear tunnelling reaction mechanism quite accurately. As testified by the fact that theory provides, within experimental errors, an overall account of the absolute differential cross sections for a rather large sample of the available transfer data, one can posit that the 2nd–order DWBA two–nucleon transfer reaction mechanism including successive, simultaneous and non–orthogonality contributions, provides a quantitative description of single Cooper pair nuclear tunnelling.

~~6. Searching for the sources of BCS condensation in nuclei: measuring phonon induced pairing with single Cooper pair transfer~~

The $N = 6$ isotope of $^{9}_{3}$Li displays quite ordinary structural properties and can, at first glance, be thought of a two–neutron hole system in the $N = 8$ closed shell. That this is not the case emerges clearly from the fact that ^{10}Li is not bound, the lowest virtual $(1/2^{+})$ and resonant $(1/2^{-})$ states testifies to the fact that, in the present case, the $N = 6$ is a far better

6.1 Dressing of single-particle states; parity inversion in ^{10}Li

(essentially PO self-energy through processes)

12

continuum state

The coupling of the $s_{1/2}$ to the different vibrations of the ^9Li core lowers its energy

magic neutron number ~~in the present case~~ than $N = 8$. Furthermore, that the unbound $s_{1/2}$ state lies lower than the unbound $p_{1/2}$ state, in plain contradiction with *static* mean field theory.

¶ Dressing the (standard) mean field single–particle state with vibrations (~~dynamic shell model, see e.g.[52] and refs. therein~~), mostly with the core quadrupole vibration, through polarization (effective mass–like) and correlation diagrams (vacuum zero point fluctuations (ZPF)) diagrams, similar to those associated with the (lowest order) Lamb shift Feynman diagrams), move the $s_{1/2}$ and $p_{1/2}$ mean field levels around. In particular the $1p_{1/2}$ from a bound state (≈ -1.2MeV), to a resonant state lying at ≈ 0.5MeV (Pauli principle, vacuum ZPF process), ~~and the $s_{1/2}$ continuum state down~~ to an ~~essentially~~ bound, virtual ~~stable~~ (~~self-energy-like diagrams~~), ~~as shown in ref.[53] (see also the contribution of Broglia~~ to this ~~volume~~).

, cf. App. C

see Fig. 5.3 (I)

almost

state lying below the $p_{1/2}$ resonance

~~Adding one further nucleon leads to a bound system. In fact, $^{11}_{3}Li_8$ displays a two-neutron separation energy $S_{2n} \approx 400$keV. A NFT description of this system which provides~~

as predicted making use of a standard mean field potential,

in keeping with the fact that the quadrupole vibration of the ^9Li core has as main component the $(p_{1/2}, p_{3/2}^{-1})_{2^+}$ neutron configuration,

(e) How can one check that CO and PO like processes as ~~like~~ the ones shown in Fig. 6.3 (cf. also Fig 6.B.1) are the basic processes dressing the odd neutron of ^{10}Li, and thus the mechanism at the basis of parity inversion? The answer is, forcing these virtual processes to become real. While this is not easy to accomplish in one-particle transfer processes involving the unbound states, $s_{1/2}$ and $p_{1/2}$, ^{10}Li virtual and resonant states, it can done with the help of two-particle transfer processes, namely that associated with inverse kinematics (p,t) reaction ^{1}H(^{11}Li, ^{9}Li(2.69 MeV; $1/2^-$))^{3}H (cf. Fig. 6.4 and Chs. 7 and 8). The price to pay for not being able to use the specific probe of single-particle modes (one-particle transfer), is ~~that~~ of adding to the self-energy contributions in question those corresponding to vertex corrections (cf. Fig. 6.4(d); for details cf. Sect 8.1 (application 2n-transfer)).

Within the present context, it is difficult, if not impossible to talk about single-particle motion without also referring to collective vibrational states (cf. e.g. Fig. 6.3(I)) both in structure and reactions, as well as to talk about pair addition and pair substraction correlations, without at the same time talking about vibrations and dressed (quasiparticle) motion (see e.g. Fig. 6.4 (a) and b). And this again in structure and reactions.

Within the framework of the present

(f) Such a reaction is feasible, (see Fig. 6.3 (II)) in keeping with the fact that, ~~In fact,~~ adding a neutron to ^{10}Li leads to a bound state. In fact, $^{11}_{3}Li_{8}$ displays a two-neutron separation energy $S_{2n} \approx 400$ keV (for further details we refer to Ch. 8, Sect. 8.1.1). (f)

monograph, the above facts imply ~~that~~ 15
chapters 5 (inelastic), 6 (one-particle transfer)
and 7 and 8 (two-particle and applications ~~transfer~~) form a
higher unity. The unity extending also
to Ch. 9 (knock-out reactions), if one also
considers the question of final state interactions, and
thus of the possibility that ~~the direct process~~
~~depicted in Fig 6.3(d) receives contribution~~
~~from~~ of the population of the state $1/2^-$
depicted in Fig. 6.4 (a), received contributions
other, and more involved, than those associa-
ted with the direct two-nucleon pick-up
depicted (for details cf. Ch. 8).

e

to p. 16

Fig. 5
Potel + Broglia

6.2.2 The ~~single-particle state of~~ ^{11}Be and phonon renormalization effects

6.3 $^{132}Sn(d,p)^{133}Sn$, $^{132}Sn(p,d)^{131}Sn$

6.4 $^{120}Sn(p,d)^{119}Sn$, $^{120}Sn(d,p)^{121}Sn$

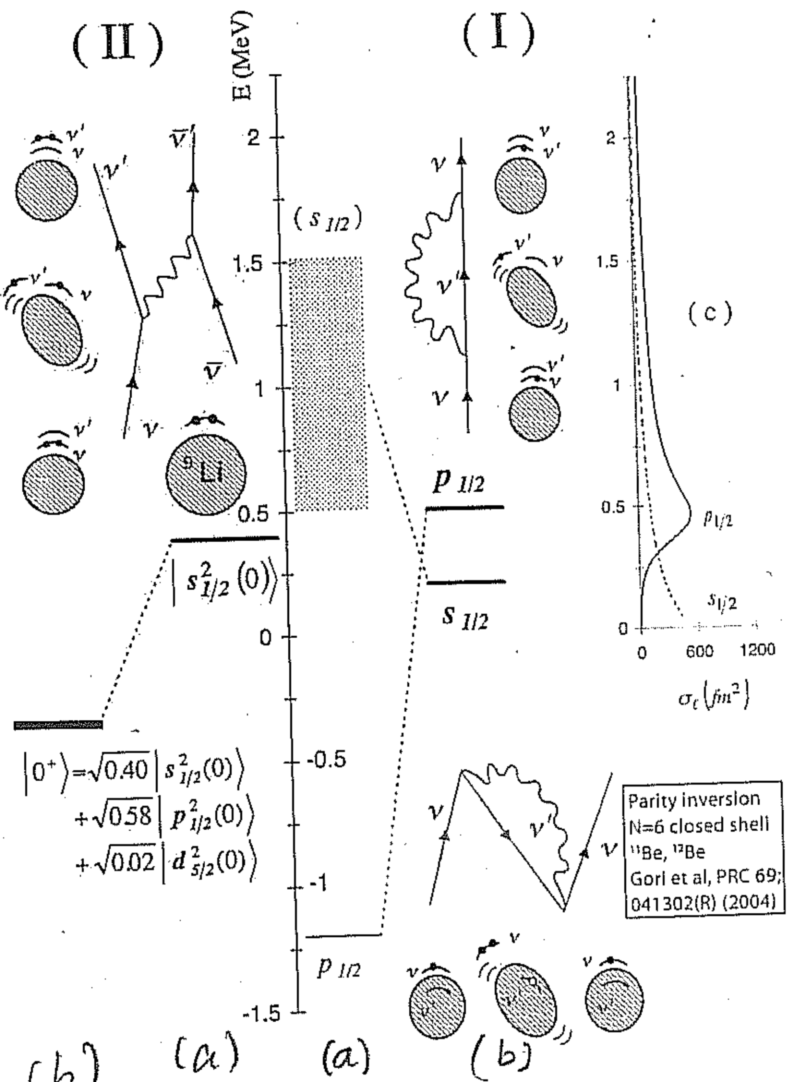

~~Barranco et al, EPJ A11 (2001) 305~~

~~Figure 3.~~

Fig. 6.3

see Fig. articolo originale EPJA 11 (2001) 305

see Ch 6 caption next page 16a

16 a

tion energy in ^{11}Li is only $S_{2n} = 0.294 \pm 0.03$ MeV [7] as compared with values of 10 to 30 MeV in stable nuclei, c) ^{10}Li displays s- and p-wave resonances at low energy, their centroids lying within the energy range 0.1–0.25 MeV and 0.5–0.6 MeV, respectively [16], while these orbitals, in particular the $p_{1/2}$ level, are well bound in nuclei of the same mass lying along the stability valley, d) the mean-square radius of ^{11}Li, $\langle r^2 \rangle^{1/2} = 3.55 \pm 0.10$ fm [17–19], is very large as compared to the value 2.32 ± 0.02 fm of the ^{9}Li core, and testifies to the fact that the neutron halo must have a large radius ($\approx$ 6–7 fm), e) the momentum distribution of the halo neutrons is found to be exceedingly narrow, its FWHM being equal to $\sigma_\perp = 48 \pm 10\,\mathrm{MeV}/c$ for the (perpendicular) distribution observed in the case of the break-up of ^{11}Li on ^{12}C, a value which is of the order of one fifth of that measured during the break-up of normal nuclei [6,7], f) the ground state of ^{11}Li is a mixture of configurations where the two halo nucleons move around the ^{9}Li core in s^2- and p^2-configurations with almost equal weight [20,21], the wave functions of the two-particle–like normal nuclei, although being strongly mixed are, as a rule, dominated by a single two-particle configuration.

Before discussing the sources of pairing correlations in ^{11}Li, we shall study the single-particle resonant spectrum of ^{10}Li. The basis of (bare) single-particle states used was determined by calculating the eigenvalues and eigenfunctions of a nucleon moving in the mean field of the ^{9}Li core, for which we have used a Saxon-Woods potential parametrized as in refs. [2,22] (cf. [2], Vol. I, eqs. (2-181), (2-182); [22], eq. (3.48)), leading to a depth $V = 51 - 30(N-Z)/A$ MeV $= 41$ MeV. The continuum states of this potential were calculated by solving the problem in a box of radius equal to 40 fm, chosen so as to make the results associated with ^{10}Li and ^{11}Li discussed below, stable. While mean-field theory predicts the orbital $p_{1/2}$ to be lower than the $s_{1/2}$ orbital (cf. fig. 1, I(a)), experimentally the situation is reversed. Similar parity inversions have been observed in other isotones of $^{10}_{3}$Li$_7$, like, *e.g.* $^{11}_{4}$Be$_7$. Shell model calculations testify to the fact that the effect of core excitation, in particular of quadrupole type, play a central role in this inversion [23] (cf. also [24]). In keeping with this result, we have studied the effect the coupling of the $p_{1/2}$ and $s_{1/2}$ orbitals of ^{10}Li to quadrupole vibrations of the ^{9}Li core has on the properties of the $(1/2^+)$ and $(1/2^-)$ states of this system (monopole and dipole vibrations display no low-lying strength and their coupling to the single-particle states of ^{10}Li lead to negligible contributions). The vibrational states of ^{9}Li were calculated by diagonalizing, in the random phase approximation (RPA), a multipole-multipole separable interaction taking into account the contributions arising from the excitation of particles into the continuum states. We adopted the self-consistent value for the coupling strength, because a calculation in the neighbor nucleus ^{10}Be yields good agreement with the experimentally known transition probability of the quadrupole low-lying vibrational state [25,26].

In the calculation of the renormalization effects of the single-particle resonances of ^{10}Li due to the coupling to vi-

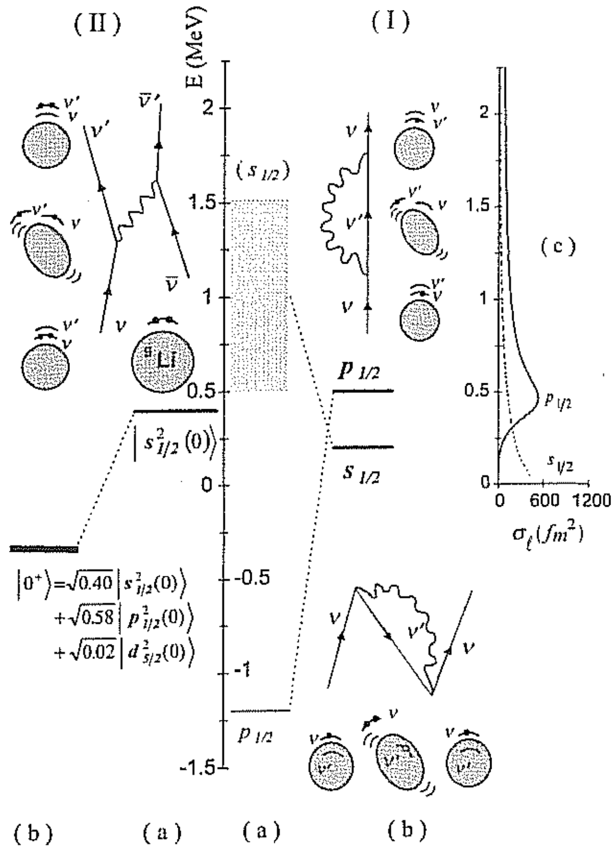

~~Fig. 1~~ Fig. 6.3. (I) Single-particle neutron resonances in ^{10}Li. In (a) the position of the levels $s_{1/2}$ and $p_{1/2}$ calculated making use of mean-field theory is shown (hatched area and thin horizontal line, respectively). The coupling of a single-neutron (upward pointing arrowed line) to a vibration (wavy line) calculated making use of the Feynman diagrams displayed in (b) (schematically depicted also in terms of either solid dots (neutron) or open circles (neutron hole) moving in a single-particle level around or in the ^{9}Li core (hatched area)), leads to conspicuous shifts in the energy centroid of the $s_{1/2}$ and $p_{1/2}$ resonances (shown by thick horizontal lines) and eventually to an inversion in their sequence. In (c) we show the calculated partial cross-section σ_l for neutron elastic scattering off ^{9}Li. (II) The two-neutron system ^{11}Li. We show in (a) the mean-field picture of ^{11}Li, where two neutrons (solid dots) move in time-reversal states around the core ^{9}Li (hatched area) in the $s_{1/2}$ resonance leading to an unbound $s^2_{1/2}(0)$ state where the two neutrons are coupled to zero angular momentum. The exchange of vibrations between the two neutrons shown in the upper part of the figure leads to a density-dependent interaction which, added to the nucleon-nucleon interaction, correlates the two-neutron system leading to a bound state $|0^+\rangle$, where the two neutrons move with probability 0.40, 0.58 and 0.02 in the two-particle configurations $s^2_{1/2}(0)$, $p^2_{1/2}(0)$ and $d^2_{5/2}(0)$, respectively. (reported with permission from Barranco et al Eur. Phys. J A11 (2001) 305, Copyright 2001, European Physical Journal)

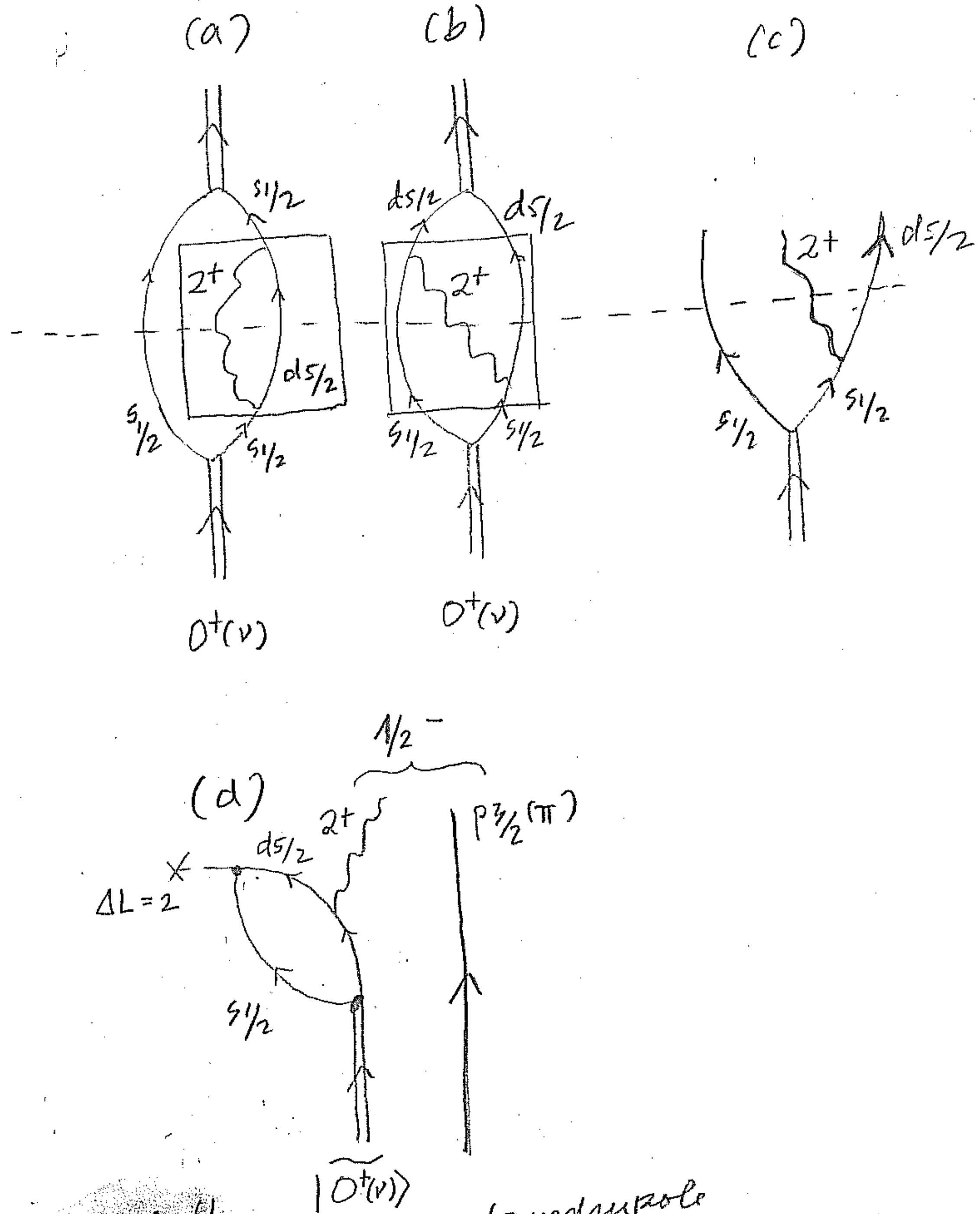

Fig. 6.4 (a) Self-energy (see boxed process) and (b) vertex (quadrupole pairing induced interaction (boxed process)) renormalization process, both associate with (c) with a (two-particle)-vibration) intermediate (virtual state) which can be forced to become real in a (p,t) reaction $^{1}H(^{11}Li,^{9}Li)^{3}H$ exciting the first excited state $|2.69 MeV; 1/2^{-}\rangle$ of ^{9}Li (see Ch. [illegible])

18

App. 6 A

~~6.5~~ Minimal requirements for a consistent mean field theory 6A.1

In what follows the question of why, rigorously speaking, one cannot talk about single–particle motion, let alone spectroscopic factor, not even within the framework of Hartree–Fock theory, is briefly touched upon.

As can be seen from Fig. ~~??~~ the minimum requirements of selfconsistency to be imposed upon single particle motion requires both non–locality in space (HF) and in time (TDHF),

$$i\hbar\frac{\partial\rho_\nu}{\partial t} = -\frac{\hbar^2}{2m}\nabla^2\varphi_\nu(x,t) + \int dx'dt'\,U(x-x',t-t')\varphi_\nu(x',t') \qquad (6A.1)\ ~~(6.61)~~$$

and consequently also of collective vibrations and, consequently, from their interweaving to dressed single–particles (quasiparticles), let alone renormalized collective modes. Assuming for simplicity infinite nuclear matter (confined by a constant potential of depth V_0), and thus plane wave solutions, the above time–dependent Schrödinger equation leads to the quasiparticle dispersion relation ~~(cf. e.g. ??)~~ (Cf. e.g. Brink and Broglia, Nuclear Superfluidity, Cambridge University Press, Cambridge (2005) App. B)

$$\hbar\omega = \frac{\hbar^2k^2}{2m^*} + \frac{m}{m^*}V_0, \qquad (6A.2)\ ~~(6.62)~~$$

where the effective mass

$$m^* = \frac{m_k m_\omega}{m}, \qquad (6A.3)\ ~~(6.63)~~$$

19

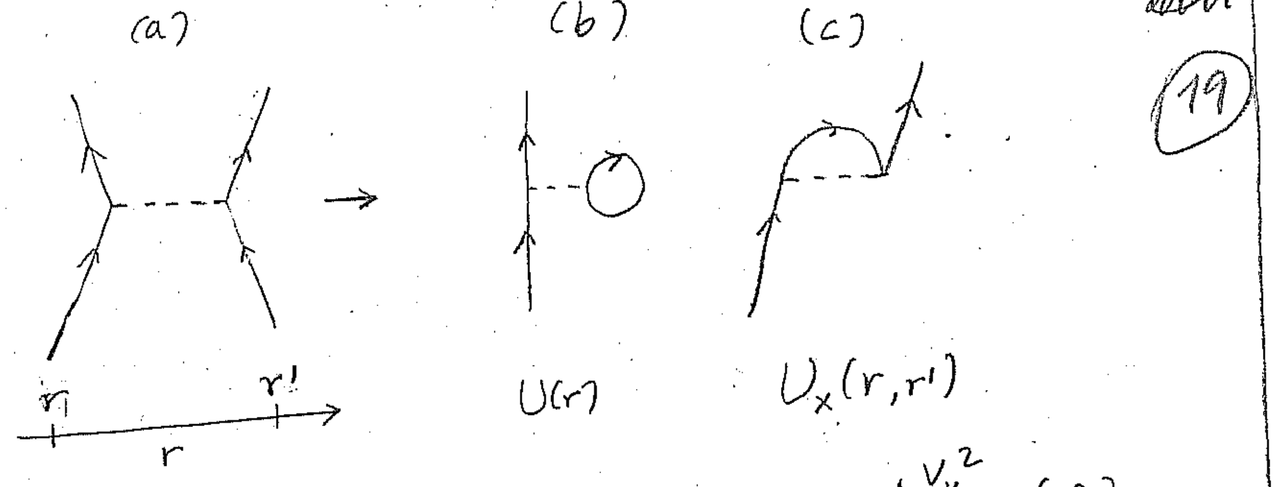

(d) $U(r) = \int d^3r\, \rho(r')\, v(|\vec{r}-\vec{r}'|)$

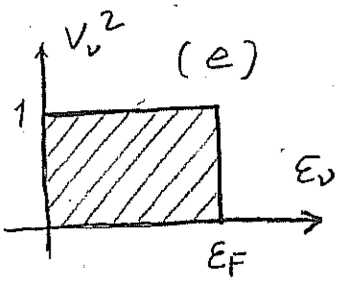

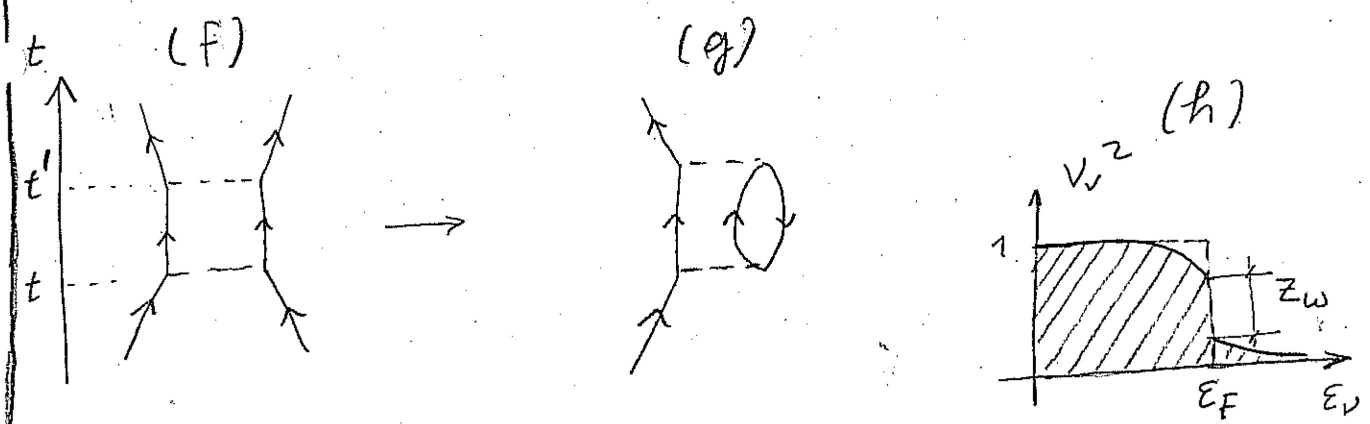

(i) $\delta U(r) = \int d^3r\, \delta\rho(r')\, v(|\vec{r}-\vec{r}'|)$

Fig.6A.1 (a) Scattering of two nucleons through the bare NN interaction $v(|\vec{r}-\vec{r}'|)$, (b) contribution to the direct (U, Hartree) and (c) to the exchange (U_x, Fock) potential, resulting in (d) the (static) selfconsistent relation between potential and density, which (e) uncouples occupied ($\varepsilon_\nu \leq \varepsilon_F$) from empty states ($\varepsilon_\nu > \varepsilon_F$). (f) multiple scattering of two nucleons lead, through processes like the one depicted in (g), eventually propagated to all orders, to: (h) a softening of the discontinuity of the occupancy of levels at ε_F, as well as to: (i) generalization of the static selfconsistency into a dynamic relation encompassing also collective vibrations (Time-dependent HF solutions of the nuclear Hamiltonian, conserving energy weighted sum rules (EWSR)) of Eq. (6A.1) (see Figs 6A.1(a) and (i)) remind very much those associated with the solution

20

más grande ecuaciones y texto

in the product of the k–mass

$$m_k = m\left(1 + \frac{m}{\hbar^2 k}\frac{\partial U}{\partial k}\right)^{-1} \qquad \text{(6A.4)} \quad \cancel{(6.64)}$$

closely connected with ~~the~~ Pauli principle $\left(\frac{\partial U}{\partial k} \approx \frac{\partial U_x}{\partial k}\right)$, while the ω–mass

$$m_\omega = m\left(1 - \frac{\partial U}{\partial \hbar\omega}\right) \qquad \text{(6A.5)} \quad \cancel{(6.65)}$$

(6A.2)

results from the dressing of ~~the~~ nucleons through the coupling with ~~the~~ (quasi) bosons. Because typically $m_k \approx 0.7m$ and $m_\omega \approx 1.4m$ $m^* \approx m$, one could be tempted to conclude that the results embodied in the dispersion relation ~~??~~ 6A.1(h) reflects the fact that the distribution of levels around the Fermi energy can be described in terms of the solutions of a Schrödinger equation in which nucleons of mass equal to the bare nucleon mass m move in a Saxon–Woods potential of depth V_0.

Now, it can be shown that the occupancy of levels around ε_F is given by Z_ω (cf. Fig. ~~??~~) a quantity which is equal to $m/m_\omega \approx 0.7$. This, in keeping with the fact that during the time the nucleon is coupled to the vibrations, it cannot behave as a single–particle and can thus not contribute to e.g. the single–particle pickup cross section.

It is of notice that the selfconsistence requirements for the iterative solution of the Kohn–Sham equations

$$H^{KS}\varphi_\gamma(\mathbf{r}) = \lambda_\gamma\varphi_\gamma(\mathbf{r}), \qquad \text{(6A.6)} \quad \cancel{(6.66)}$$

where

$$H^{KS} = -\frac{\hbar^2}{2m_e}\nabla^2 + U_H(\mathbf{r}) + V_{ext}(\mathbf{r}) + U_{xc}(\mathbf{r}), \qquad \text{(6A.7)} \quad \cancel{(6.67)}$$

H^{KS} being known as the Kohn–Sham Hamiltonian, $V_{ext}(\mathbf{r})$ ~~being~~ denoting the field created by the ions and acting on the electrons. Both the Hartree and the exchange–correlation potentials $U_H(\mathbf{r})$ and $U_{xc}(\mathbf{r})$ depend on the (local) density, hence on the whole set of wavefunctions $\varphi_\gamma(\mathbf{r})$. Thus, the set of KS–equations must be solved selfconsistently. ~~??~~ (Broglia, Colò, Onida and Roman, Solid state physics of finite systems, Springer-Verlag Heidelberg (2004) Ch. 3)

write

App. 6B ~~6.6~~ Model for single–particle strength function: Dyson equation

lower case

In the previous section we introduced the argument of the ~~impossibility~~ difficulty of defining a "bona fide" single–particle spectroscopic factor. It was done with the help of Feynman (NFT) diagrams. In what follows we essentially repeat the arguments, but this time in terms of Dyson's (Schwinger) language.

For simplicity, we consider a two–level model where the pure single–particle state $|a\rangle$ couples to a more complicated state $|\alpha\rangle$, made out of a fermion (particle or hole), couple to a particle–hole excitation which, if iterated to all orders can give rise to a collective state (cf. Fig. ~~??~~). The Hamiltonian describing the system is

$$H = H_0 + \cancel{U}\, v \qquad \text{(6B.1)} \quad \cancel{(6.68)}$$

where

$$H_0|a\rangle = E_a|a\rangle, \qquad \text{(6B.2)} \quad \cancel{(6.69)}$$

6B.1: see also Brink and Satchler (2005) App. D

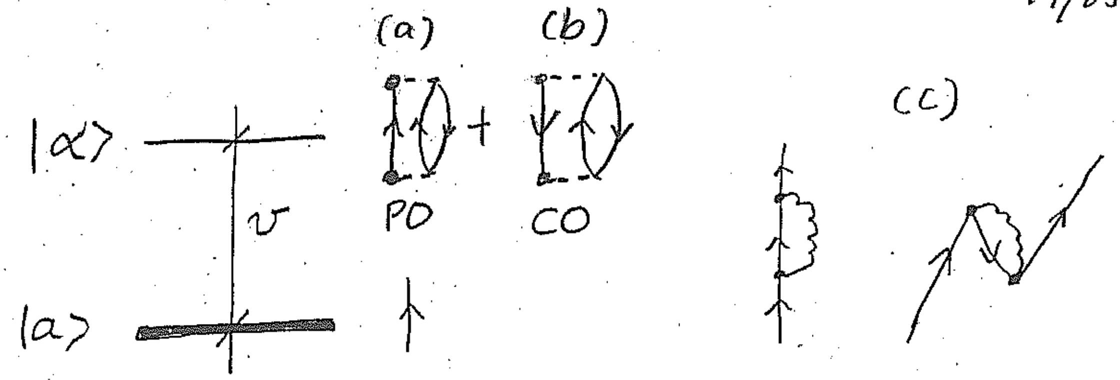

Fig. 6B.1

Two state schematic model describing the breaking of the strength of the pure single-particle state |a>, through the coupling to collective vibrations (wavy line) associated with polarization (PO) and correlation (CO) processes.

App. 6C. Self-energy and vertex corrections

and

$$H_0|\alpha\rangle = E_\alpha|\alpha\rangle. \qquad \cancel{(6.70)}\ (6B.3)$$

Let us call $\langle a|\overset{v}{\cancel{U}}|\alpha\rangle = \overset{v}{\cancel{U}}_{a\alpha}$ and assume $\langle a|\cancel{U}|a\rangle = \langle\alpha|\overset{v}{\cancel{U}}|\alpha\rangle = 0$.

From the secular equation ~~associated with H, namely~~

$$\begin{pmatrix} E_\alpha & U_{a\alpha} \\ U_{a\alpha} & E_a - E_i \end{pmatrix}\begin{pmatrix} C_\alpha(i) \\ C_a(i) \end{pmatrix} = 0, \qquad \cancel{(6.71)}\ (6B.4)$$

and associated normalization condition

$$C_a^2(i) + C_\alpha^2(i) = 0, \qquad \cancel{(6.72)}\ (6B.5)$$

one obtains

$$C_a^2(i) = \left(1 + \frac{\overset{v}{\cancel{U}}{}^2_{a\alpha}}{(E_\alpha - E_i)^2}\right)^{-1}, \qquad \cancel{(6.73)}\ (6B.6)$$

and

$$\Delta E_a(E) = E_a - E = \frac{\overset{v}{\cancel{U}}{}^2_{a\alpha}}{E_a - E}. \qquad \cancel{(6.74)}\ (6B.7)$$

The energy of

~~The relations 6.73 and 6.74 allows one to write~~ the correlated state

(6B.7)

$$|\tilde{a}\rangle = C_a(i)|a\rangle + C_\alpha(i)|\alpha\rangle, \qquad \cancel{(6.75)}\ (6B.8)$$

is obtained

~~the corresponding energy being provided~~ by the (iterative) solution of the Dyson equation ~~6.74~~, which propagates the bubble diagrams shown in Figs. ~~??~~ (a) and (b) to infinite order leading to collective vibrations (see Fig. ~~??~~). 6B.1

With the help of the definition ~~??~~, and making use of the fact that in the present case, $U \equiv \Delta E_a(E)$, one obtains 6B.1(c)

(of the relation given in Eq.(6B.7))

$$Z_\omega = C_a^2(i) = \frac{m_\omega}{m} \qquad \cancel{(6.76)}\ [6B.9]$$

given in Eqs.(6B.5) and (6B.6),

the solution of ~~6.74~~ together with the relations ~~?? and ??~~ lead to the quasiparticle state ~~??~~, to be employed in the calculation of the one–particle transfer transition amplitudes ~~(cf. e.g. ?? and ??)~~

(6B.8)

Making use of

given in Eq.(6A.5)

App. 6C Self-energy and vertex corrections

In Fig. 6C.1 an example of the fact that in field theories (e.g. QED or NFT), ~~that~~ nothing is free and that e.g. the bare mass of a fermion (electron or nucleon) is the parameter one adjusts (mk) so that the result of a measurement (cf. Fig. 6C.1) gives the observed mass (single-particle energy). In Fig 6C.2, lowest order diagrams associated with the renormalization of the fermion-boson interaction (vertex corrections) are given. The sum of contributions (a) and (b) can, in principle, be represented by a renormalized vertex (cf. diagram (c) of Fig. 6C.2). It is of notice, however, that there is, as a rule, conspicuous interference (e.g. cancellation ~~tion~~ in the nuclear case between vertex and self-energy contributions (cf. diagram (e) and (f) of Fig. 6C.2)). In particular, cancellation in the case in which the bosonic modes are isoscalar (a phenomenon closely related with conservation laws (generalized Ward identities)). Consequently, one has to sum explicitely the different amplitues with the corresponding phases and eventually take the modulus squared of the result, to eventually obtain the quantities to be compared with the data, a fact that preclude the use of an effective (renormalized) vertex (cf. Fig. 6C.2 (c)).

Within the framework of QED (the above mentioned) cancellations are exact implying ~~that~~ the interaction between one and two photon state vanishes (Furry theorem).

The ~~basic~~ physics at the (isoscalar) basis of the cancellation found in the nuclear case, can be exemplified by looking at a spherical nucleus displaying a low-lying collective quadrupole vibration. The associated zero point fluctuations (ZPF) lead to time dependent shapes with varied instantaneous values of the quadrupole moment, and of its orientation (dynamical spontaneous breaking of rotational invariance). In other words, a component of the ground state wavefunction $(|(j_p \otimes j_h^{-1})_{2^+} \otimes 2^+; 0^+\rangle)$ can be viewed as a gas of quadrupole (quasi) bosons. ~~correlated particle hole coupled~~ ~~Because~~ Promoting a nucleon across the Fermi energy (particle-hole excitation) will lead to ~~fermionic~~ excitation states which behave has having a positive ~~quadru~~ (particle) and a negative (hole) effective quadrupole moment, inkeeping with the ~~fact that~~ the closed shell system is spherical, thus carrying zero quadrupole moment.

Self-Energy (effective mass) processes

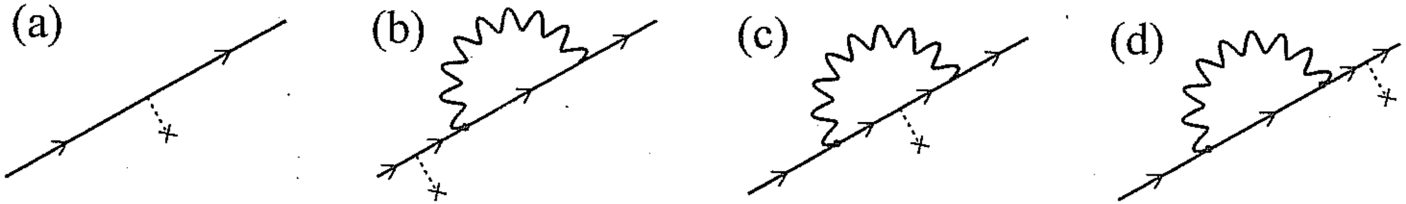

Fig.6C.1

Fig. 6C.1 :The result of the probing with an external field (dotted line started with a cross) of the properties (mass,single-particle energy,etc) of a fermion (e.g. an electron or a nucleon,arrowed line) dressed through the coupling of (quasi) bosons (photons or collective vibrations,wavy line), corresponds to the modulus squared of the sum of the amplitudes associated with each of the four diagrams (a)-(d) (cf. R.P. Feynman, Theory of fundamental processes).

25
a

Vertex corrections

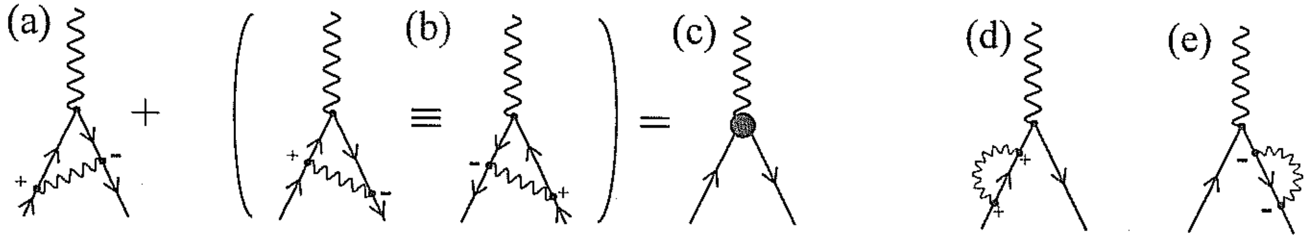

Fig 6C,2

125 b

Fig 6C.2: These are ~~triple~~-interaction vertex diagrams in which none of the incoming lines can be detached ~~###~~ from either of the other two by cutting one line. Midgal's (1958) theorem states that, for phonons and electrons (Bardeen-Pines-Frölich mechanism to break gauge invariance), vertex corrections can be neglected, but usually they are not negligible, in any case not in nuclei (cancellation) (cf. e.g. P.W. Anderson, Basic notions of condensed matter physics). The solid circle in (c) represents the effective, ~~vertex~~ renormalized vertex.

25 c

6C.1 The Lamb Shift

In Fig. 6C.3 we display a schematic summary of the electron-photon processes, associated with Pauli principle corrections, leading to the splitting of the lowest s,p state of the hydrogen atom known as the Lamb shift.

In the upper part of the Figure the predicted position of the electronic single-particle levels of the hydrogen atom as resulting from the solution of the Schrödinger equation (Coulomb field). In the lowest part of the figure, one displays the electron of an hydrogen atom (upwardsgoing arrowed line) in presence of vacuum ZPF (electron-positron pair plus photon, oyster-like diagram). Because the associate electron virtually occupies states already occupied by the hydrogen's electron, thus violating Pauli principle, one has to antisymmetrized the corresponding two-electron state. Such process gives rise to the exchange of the corresponding fermionic lines and thus to CO-like diagrams as well as, through time ordering, to PO-like diagrams. The results provide a quantitative account of the experimental findings.

~~Virtual processes become real: II~~

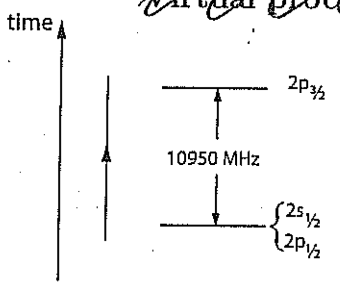

W.E. Lamb, Jr., R.C. Retherford,
Phys. Rev. 72 (1947) 241

(1 MeV: 2.42 10^8 MHz)

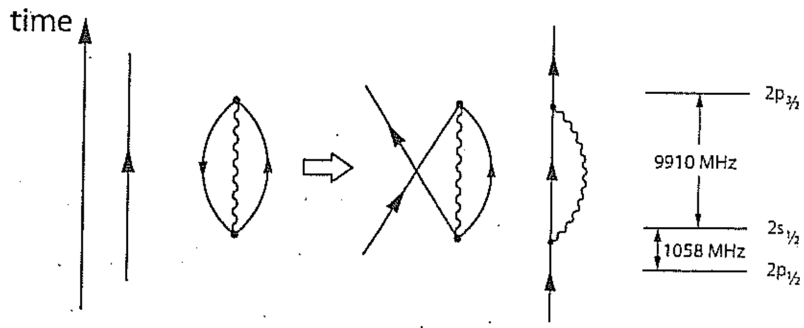

breaking of the s,p level degeneracy

~~W. Pauli, 1945 Nobel lecture, Neuchatel (1947)~~

~~$\frac{e^2}{\hbar c} \approx \frac{1}{137}$ fine structure constant~~

~~Nothing is free ... and the bare mass is the parameter you adjust to get the observed mass once renormalization has been done (R.P. Feynman)~~

~~Increasing importance as medium polarization increases atoms → nuclei → halo~~

~~Figure 1.~~

Caption

Fig. 6C.2

Schematic representation of the processes associated with the Lamb shift.

App. 6D singe-nucleon transfer for pedestrians

(27)

~~6.3 No–recoil, local, plane wave limit~~

In this Appendix we discuss some aspects of the relation existing between nuclear structure and one–particle transfer cross sections. To do so, we repeat some of the steps carried out in the text but this time in ~~the most~~ a more simple and straightforward way, ignoring the complications ~~associated~~ with the spin carried out by the particles, the spin–orbit ~~dependence~~ of the optical model potential, the recoil effect, etc. We consider the case of $A(d,p)A+1$ reaction, namely that of neutron stripping. The intrinsic wave functions ψ_α and ψ_β, where $\alpha = (A,d)$ and $\beta = ((A+1),p)$,

$$\psi_\alpha = \psi^{I_A}_{M_A}(\xi_A)\phi_d(\vec{r}_{np}), \qquad (6D.1)\ \text{~~(6.37a)~~}$$

$$\begin{aligned}\psi_\beta &= \psi^{I_{A+1}}_{M_{A+1}}(\xi_{A+1}) \\ &= \sum_{l,I'_A}(I'_A;l|\}I_{A+1})[\psi^{I'_A}(\xi_A)\phi^l(\vec{r}_n)]^{I_{A+1}}_{M_{A+1}-M_A},\end{aligned} \qquad (6D.2)\ \text{~~(6.37b)~~}$$

where $(I'_A;l|\}I_{A+1})$ is a generalized fractional parentage coefficient. It is of notice that this fractional parentage expansion is not well defined. In fact, as a rule, $(I'_A;l|\}I_{A+1})\phi^l(\vec{r}_n)_{M_{A+1}-M_A}$ is an involved, dressed quasiparticle state ~~containing only a~~ fraction of the "pure" single particle strength (cf. ~~27~~ Cf. app. 6A and app. 6B). For simplicity we assume the expansion is operative. To further simplify the derivation we assume we are dealing with spinless particles. The variable $\vec{r}_{np}$ is the relative coordinate of ~~the proton and the~~ neutron (see Fig. ~~22~~ 6D.1).

The transition matrix element can now be written as

$$\begin{aligned}T_{d,p} &= \langle\psi^{I_{A+1}}_{M_{A+1}}(\xi_{A+1})\chi^{(-)}_p(k_p,\vec{r}_p), V'_\beta\psi^{I_A}_{M_A}(\xi_A)\chi^{(+)}_d(k_d,\vec{r}_d)\rangle \\ &= \sum_{l,I'_A,M'_A}(I'_A;l|\}I_{A+1})(I'_A\,M'_A\,l\,M_{A+1}-M'_A|I_{A+1}\,M_{A+1}) \\ &\times\int d\vec{r}_n d\vec{r}_p\chi^{*(-)}_p(k_p,\vec{r}_p)\phi^{*l}_{M_{A+1}-M'_A}(\vec{r}_n)(\psi^{I_A}_{M_A}(\xi_A),V'_\beta\psi^{I'_A}_{M'_A}(\xi_A)) \\ &\times\phi_d(\vec{r}_{np})\chi^{(+)}_d(k_d,\vec{r}_d)\,\delta_{I'_A,I_A}\,\delta_{M'_A,M_A}.\end{aligned} \qquad (6D.3)\ \text{~~(6.38)~~}$$

In the stripping approximation

$$\begin{aligned}V'_\beta &= V_\beta(\xi,\vec{r}_\beta) - \bar{U}_\beta(r_\beta) \\ &= V_\beta(\xi_A,\vec{r}_{pA}) + V_\beta(\vec{r}_{pn}) - \bar{U}_\beta(r_{pA})\end{aligned} \qquad (6D.4)\ \text{~~(6.39)~~}$$

Then

$$\begin{aligned}(\psi^{I_A}_{M_A}(\xi_A),V'_\beta\psi^{I_A}_{M_A}(\xi_A)) &= (\psi^{I_A}_{M_A}(\xi_A),V_\beta(\xi_A,\vec{r}_{pA})\psi^{I_A}_{M_A}(\xi_A)) \\ &+ (\psi^{I_A}_{M_A}(\xi_A),V_\beta(\vec{r}_{pn})\psi^{I_A}_{M_A}(\xi_A)) - \bar{U}_\beta(r_{pA}).\end{aligned} \qquad (6D.5)\ \text{~~(6.40)~~}$$

We assume

$$U_\beta(r_{pA}) = (\psi^{I_A}_{M_A}(\xi_A),V_\beta(\xi_A,\vec{r}_{pA})\psi^{I_A}_{M_A}(\xi_A)). \qquad (6D.6)\ \text{~~(6.41)~~}$$

Then

$$(\psi^{I_A}_{M_A}(\xi_A),V'_\beta\psi^{I_A}_{M_A}(\xi_A)) = V_{np}(\vec{r}_{pn}) \qquad (6D.7)\ \text{~~(6.42)~~}$$

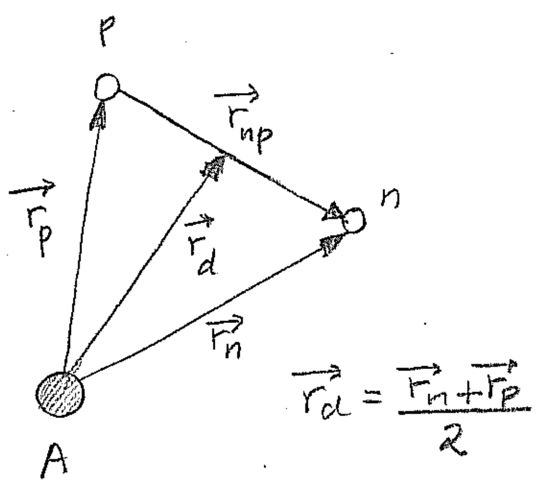

FIG 6D.1
Cordinate used in the description of the A(d,p)(A+1) stripping process.

(6D.7) (6D.3)

Inserting eq. ~~(6.42)~~ into eq. ~~(6.38)~~ we obtain

$$T_{d,p} = \sum_l (I_A; l|\}I_{A+1})(I_A\, M_A\, l\, M_{A+1} - M_A | I_{A+1}\, M_{A+1})$$

$$\times \int d\vec{r}_n d\vec{r}_p \chi_p^{*(-)}(k_p, \vec{r}_p)\phi^{*l}_{M_{A+1}-M_A}(\vec{r}_n) V(\vec{r}_{pn})\phi_d(\vec{r}_{np})\chi_d^{(+)}(k_d, \vec{r}_d) \,.$$

(6D.8) ~~(6.43)~~

The differential cross section is then equal to

$$\frac{d\sigma}{d\Omega} = \frac{2}{3}\frac{\mu_p\mu_d}{(2\pi\hbar^2)^2}\frac{(2I_{A+1}+1)}{(2I_A+1)}\frac{k_p}{k_d}\sum_{l,m_l}\frac{(I_A; l|\}I_{A+1})^2}{2l+1}|B^l_{m_l}|^2,$$

(6D.9) ~~(6.44)~~

where

$$B^l_{m_l}(\theta) = \int d\vec{r}_n d\vec{r}_p \chi_p^{*(-)}(k_p, \vec{r}_p) Y^{*l}_m(\hat{r}_n) u_{nl}(r_n) V(\vec{r}_{pn})\phi_d(\vec{r}_{np})\chi_d^{(+)}(k_d, \vec{r}_d) \,,$$

(6D.10) ~~(6.45)~~

and The relation (6D.9)

$$\phi^l_m(\vec{r}_n) = u_{nl}(r_n) Y^l_m(\hat{r}_n) \,,$$

(6D.11) ~~(6.46)~~

is the single-particle wave function of a neutron moving in the core A. For simplicity, the radial wave function $u_{nl}(r_n)$ can be assumed to be a solution of a Saxon-Woods potential of parameters $V_0 \approx 50$ MeV, $a = 0.65$ fm and $r_0 = 1.25$ fm. (6D.9)

~~Equation (6.44)~~ gives the cross section for the stripping from the projectile of a neutron that would correspond to the n[th] valence neutron in the nucleus $(A+1)$. If we now want the cross section for stripping any of the valence nutrons of the final nucleus from the projectile, we must multiply eq. ~~(6.44)~~ by n. A more careful treatment of the antisymmetry with respect to the neutrons shoes this to be the correct answer.

Finally we get

$$\frac{d\sigma}{d\Omega} = \frac{(2I_{A+1}+1)}{(2I_A+1)}\sum_l S_l\sigma_l(\theta) \,,$$

(6D.12) ~~(6.47)~~

where

$$S_l = n(I_A; l|\}I_{A+1})^2 \,,$$

(6D.13) ~~(6.48)~~

and

$$\sigma_l(\theta) = \frac{2}{3}\frac{\mu_p\mu_d}{(2\pi\hbar^2)^2}\frac{k_p}{k_d}\frac{1}{2l+1}\sum_m |B^l_m|^2 \,.$$

(6D.14) ~~(6.49)~~

The distorted wave programs numerically evaluate the quantity $B^l_{m_l}(\theta)$, using for the wave functions $\chi^{(-)}$ and $\chi^{(+)}$ the solution of the optical potentials that fit the elastic scattering, i.e.

(4.11)

$$(-\nabla^2 + \bar{U} - k^2)\chi = 0$$

(6D.9) 6D.15 ~~(6.50)~~

(see eq. ~~(22)~~). Note that if the target nucleus is even, $I_A = 0$, $l = I_{A+1}$. That is, only one l value contributes in eq. ~~(6.44)~~, and the angular distribution is uniquely given by $\sum_m |B^l_m|^2$. The l-dependence of the angular distributions helps to identify $l = I_{A+1}$. The factor S_l needed to normalize the calculated function to the data yields (assuming a good fit to the angular distribution), is known in the literature as the spectroscopic factor. It was assumed not only that it could be defined, but also that it contained all the nuclear structure information (aside from that associated with the angular distribution) which could be extracted from single–particle transfer. In other words, that it was the bridge directly connecting theory with experiment. Because nucleons are never bare, but are dressed by the coupling to collective modes (~~cf. ??~~), the spectroscopic factor

cf. App. A

(30)

Let us now discuss a technical problem.

approximation is at best a helpful tool to get order of magnitude information from one particle transfer data. There is a fundamental problem which makes the handling of integrals like that of (~~6.45~~) difficult to handle, if not numerically at least conceptually. This difficulty is connected with the so called recoil effect [1], namely the fact that the center of mass coordinate of the two interacting ~~particles~~ nuclei in entrance ($\mathbf{r}_\alpha$: $\alpha = a + A$) and exit ($\mathbf{r}_\beta$: $\beta = b + B$) channels is different. This is at variance with what one is accustomed to deal with in nuclear structure calculations, in which the Hartree potential depends on a single coordinate, as well as in the case of elastic and inelastic reactions, situations in which $\mathbf{r}_\alpha = \mathbf{r}_\beta$. When $\mathbf{r}_\alpha \neq \mathbf{r}_\beta$ we enter a rather more complex many–body problem (in particular if continuum states are to be considered) than nuclear structure practitioners ~~were~~ are accustomed to deal with, (those with which)

Of notice, however, that similar difficulties have been faced in connection with the non–local Fock (exchange) potential. As a rule, the corresponding (HF) mean field equations are rendered local making use of the k–mass approximation or within the framework of Local Density Functional Theory (DFT), in particular with the help of the Kohn–Sham equations (see ~~e.g. [?], [2]~~). Although much of the work in this field is connected ~~with the correlation~~ potential (interweaving of single–particle and collective motion), an important fraction is connected with the exchange potential.

In any case, and returning to the subject of the present appendix (App. 6A), it is always useful to be able to introduce approximations which can help the physics which is at the basis of the phenomenon under discussion (single–particle motion) to emerge in a natural way, if not to compare in detail with the experimental data. Within this context, to reduce the integral ~~6.45~~ (6D.10) it is ~~customary~~ useful to assume that the proton-neutron interaction V_{np} has zero-range, i.e.

$$V_{np}(\vec{r}_{np})\phi_d(\vec{r}_{np}) = D_0\delta(\vec{r}_{np}), \qquad \text{(~~6.51~~) (6D.16)}$$

so that B^l_m becomes equal to

$$B^l_{m_l}(\theta) = D_0 \int d\vec{r}\chi_p^{*(-)}(k_p,\vec{r})Y^{*l}_{m_l}(\hat{r})u_l(r)\chi_d^{(+)}(k_d,\vec{r}). \qquad \text{(~~6.52~~) (6D.17)}$$

~~which~~ This is a three dimensional integral, but, in fact, essentially a one–dimensional ~~integral~~ one, as the integration over the angles is simple to carry out.

6.4 Plane-wave limit

6D.15

If in eq. (~~6.50~~) we set $\bar{U} = 0$ the distorted waves becomes plane waves i.e.

$$\chi_d^{(+)}(k_d,\vec{r}) = e^{i\vec{k}_d\cdot\vec{r}}, \qquad \text{(~~6.53a~~) (6D,18a)}$$

$$\chi_d^{*(-)}(k_p,\vec{r}) = e^{-i\vec{k}_p\cdot\vec{r}}. \qquad \text{(6.53b) (6D,18b)}$$

Equation (~~6.52~~) (6D.17) can now be written as

$$B^l_m = D_0 \int d\vec{r}e^{i(\vec{k}_d-\vec{k}_p)\cdot\vec{r}}Y^{*l}_m(\hat{r})u_l(r). \qquad \text{(~~6.54~~) (6D.19)}$$

[1]While this effect could be treated in a cavalier fashion in the case of light ion reactions ($m_a/m_A \ll 1$), this was not possible in the case of heavy ion reactions, as the change in momenta involved were always sizeable.

21

The linear momentum transferred to the nucleus is $\vec{k}_d - \vec{k}_p = \vec{q}$. Let us expand $e^{i\vec{q}\cdot\vec{r}}$ in spherical harmonics, i.e.

$$\begin{aligned} e^{i\vec{q}\cdot\vec{r}} &= \sum_l i^l j_l(qr)(2l+1)P_l(\hat{q}\cdot\hat{r}) \\ &= 4\pi \sum_l i^l j_l(qr) \sum_m Y^{*l}_m(\hat{q}) Y^l_m(\hat{r}), \end{aligned}$$

(6D.20) ~~(6.55)~~

so

$$\int d\hat{r} e^{i\vec{q}\cdot\vec{r}} Y^l_m(\hat{r}) = 4\pi i^l j_l(qr) Y^{*l}_m(\hat{q}).$$

(6D.21) ~~(6.56)~~

Then

$$\begin{aligned} \sum_m |B^l_m|^2 = \sum_m |Y^l_m(\hat{q})|^2 D_0^2 16\pi^2 \times \\ \left| \int r^2 dr j_l(qr) u_l(r) \right|^2 = \\ \frac{2l+1}{4\pi} D_0^2 16\pi^2 \left| \int r^2 dr j_l(qr) u_l(r) \right|^2 . \end{aligned}$$

(6D.22) ~~(6.57)~~

Thus, the angular distribution is given by the integral $\left|\int r^2 dr j_l(qr) u_l(r)\right|^2$ If we assume that the process takes place mostly on the surface, the angular distribution will be given by $|j_l(qR_0)|^2$ where R_0 is the nuclear radius.

We then have

$$\begin{aligned} q^2 &= k_d^2 + k_p^2 - 2k_d k_p \cos(\theta) \,, \\ &= (k_d^2 + k_p^2 - 2k_d k_p) + 2k_d k_p (1 - \cos(\theta)) \,, \\ &= (k_d - k_p)^2 + 4k_d k_p (\sin(\theta/2))^2 , \\ &\approx 4k_d k_p (\sin(\theta/2))^2 , \end{aligned}$$

(6D.23) ~~(6.58)~~

since $k_d \approx k_p$ for stripping reactions at typical energies. Thus the angular distribution has a diffraction-like structure given by

$$|j_l(qR_0)|^2 = j_l^2(2R_0 \sqrt{k_d k_p} \sin(\theta/2)).$$

(6D.24) ~~(6.59)~~

The function $j_l(x)$ has its first maximum at $x = l$, i.e. where

$$\sin(\theta/2) = \frac{l}{2R_0 k}, \qquad (k_p \approx k_d = k),$$

(6D.25) ~~(6.60)~~

Examples of the above relation are provided in Fig. ~~22~~ 6D.2 ,

6.5 Minimal requirements for a consistent mean field theory

In what follows th question of why, rigorously speaking, one cannot talk about single–particle motion, let alone spectroscopic factor, not even within the framework of Hartree–Fock theory, is briefly touched upon.

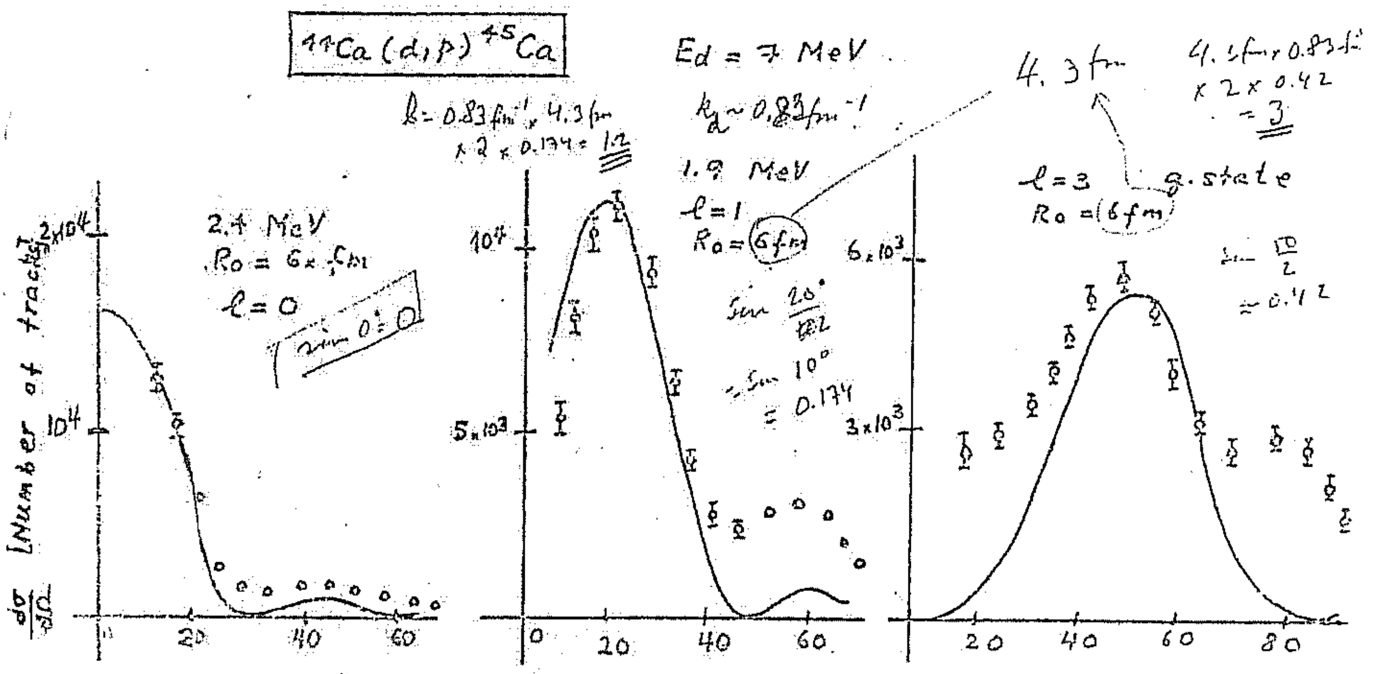

Ī : experimental value from W.R. Cobb and D.B Guth, Phys. Rev. 107, 181 (1957).
—— : plane wave estimate

~~Figure 6.2:~~

Fig 6D.2

D.B. Guth, Phys. Rev. 107, 181 (1957)